THE JOURNAL OF PHYSICAL CHEMISTRY C

ACS AUTHORCHOICE

pubs.acs.org/JPCC Article

The Elusive Nature of Carbon Nanodot Fluorescence: An Unconventional Perspective

Marcello Righetto,* Francesco Carraro, Alberto Privitera, Giulia Marafon, Alessandro Moretto, and Camilla Ferrante*

Cite This: J. Phys. Chem. C 2020, 124, 22314−22320

Read Online

ACCESS | Metrics & More | Article Recommendations | Supporting Information

ABSTRACT: The burgeoning interest raised by carbon dots (CDs) is an epitome of the urgency to develop green and biocompatible alternatives to inorganic and hybrid quantum dots. The fast-paced development of synthetic approaches for CDs over the past few years has left many open questions on their characterization. Herein, we further confirm how the standardization of CDs cannot disregard the presence of fluorescent molecular byproducts. On the contrary, we show how the emissive properties of our solvothermally synthesized CDs largely stem from free molecular adducts produced during the synthesis of carbon cores. The presence of these small molecules, not detectable by electron microscopy, could be deceptive for a reliable characterization of the CDs and could lead to an overestimate of their optical properties. Hence, we propose to introduce more bias-free structure−property correlations based on spectroscopy techniques capable of giving direct insights into their structural properties. Through a combination of standard and unconventional characterization techniques, such as fluorescence correlation spectroscopy (FCS) and time-resolved electron paramagnetic resonance (TREPR), we demonstrate how molecular byproducts dominate the emission properties: these are freely moving in the solution rather than decorating a carbonaceous scaffold. Considering carefully the possibility that newly synthesized CDs are heterogeneous solutions will boost the research and optimization of CDs, thereby paving the way to the large-scale production of cheap and biocompatible light-emissive nanostructures.

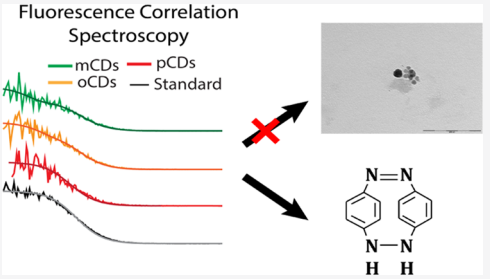

INTRODUCTION

The quest for a cheaper and greener alternative to inorganic quantum dots lies at the heart of the recent success of carbon dots (CDs).[1,2] During the past few years, record high and excitation wavelength-dependent quantum yields (QY),[3] size-tunable optical properties,[4] and versatile surface chemistry analogous to inorganic QDs have been reported for bottom-up-synthesized CDs.[5−8] Since their discovery, research has aimed to obtain highly efficient CDs emitters, thereby envisioning a wealth of applications in bioimaging, catalysis, and light-emitting devices.[9−11] The collective effort among the scientific community in the pursuit of higher QYs for CDs led to the discovery of different synthetic strategies, e.g., hydrothermal, solvothermal, and microwave-assisted syntheses.[12,13] In fulfillment of the high expectations, these systems were used to fabricate CD-based devices, reporting state-of-the-art efficiencies, and hence further fueling the interest around them.[14−16]

Despite the success of CDs, their peculiar photophysics based on substantial Stokes shifts and excitation energy-dependent photoluminescence (PL) is still highly debated within the scientific community.[17−21] Recently, a handful of groups, including our group, reported on the essential role played by molecular fluorophores in the emission properties of CDs.[22−25] Such molecular entities are produced during the pyrolysis of organic precursors in CD syntheses.[26−28] Among others, CDs synthesized by citric acid and ethylenediamine are the most paradigmatic examples of the inherent complexity of the emission properties of CDs. These CDs exhibit a sharp absorption band, high QY values, and excitation-independent PL excited through that band.[29] Nevertheless, excitations on the red tail of the absorption spectrum produce excitation-dependent PL effects, widely recognized as the hallmark of CDs' emission. Albeit different models were proposed to account for the observed emission properties (i.e., energy transfer among different fluorophores embedded within a carbonaceous scaffold, surface-mediated PL, aggregation-mediated PL),[30−32] the discovery of the highly emissive citrazinic acid derivative imidazo[1,2-*a*] pyridine-7-carboxylic acid, 1,2,3,5-tetrahydro-5-oxo (IPCA) as a byproduct of this synthesis cast doubt on the nature of this emission.[22] Recently, using fluorescence correlation spectroscopy (FCS), we demonstrated that emission of these systems originates mainly

Received: July 30, 2020
Revised: September 13, 2020
Published: September 14, 2020

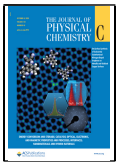

https://dx.doi.org/10.1021/acs.jpcc.0c06996
J. Phys. Chem. C 2020, 124, 22314−22320

from single IPCA molecules dispersed in solution, rather than the aforementioned molecular scaffolds or carbonaceous cores to which the chromophore is attached.[25,33]

Although carbon cores are effectively produced and observed by TEM, free IPCA molecules induce the overestimation of their QY values. Contextually, other groups reported similar findings and contributed to depicting the citric acid-based CDs as complex systems in which simple molecules and carbon cores do coexist and contribute to emission. Some recent work put into question even the nature of carbon cores, relating them to supramolecular aggregates of IPCA on TEM grids.[24,26,27]

Despite doubts cast on the whole field, these crucial investigations focused only on citric acid-based CDs, produced by the microwave method.[23−26,34] Given both the peculiar synthetic procedure and precursor chemistry, the outreach of these studies did not impact the whole field of carbon dots. Here, we provide a broader view on the emission properties of CDs by studying CDs synthesized using different precursors (i.e., precursors with different chemical reactivities) and using conventional solvothermal synthesis, aiming to provide conclusions of more general significance for the field of CDs. Furthermore, in compliance with most recent reports on the purification of CDs,[35] we carried out a thorough purification procedure. Results indicate that the generation of molecular fluorophores is a widespread phenomenon potentially extending to all CDs, thus necessitating a critical reconsideration of past and future studies on CD emission.

EXPERIMENTAL METHODS

Synthesis and Characterization of Carbon Nanodots. Three different CDs were synthesized closely following the procedures reported in Ref 4. Briefly, 8.5 mmol of ACS reagent-grade para-phenylenediamine (Aldrich) was dissolved in ethanol (90 mL) and transferred in autoclaves. The solution was heated to 180 °C for 12 h in an oven, producing a dark crude dispersion of *p*CDs. A similar procedure was adopted for *ortho*- and *meta*-phenylenediamine (Aldrich) to obtain *o*CDs and mCDs, respectively. The resulting solution of CDs was then purified with silica column chromatography using highly polar mixtures of dichloromethane and methanol as eluents. TEM micrographs were obtained using a CM 12 PHILIPS TEM operating at 120 kV on drop-cast amorphous carbon-coated Cu grids for as-synthesized CD mixtures.

X-ray Photoemission Spectroscopy (XPS). X-ray photoelectron spectroscopy (XPS) spectra were collected in an ultra high vacuum chamber equipped with an EA 125 Omicrom electron analyzer. Core-level photoemission spectra (C 1s and N 1s regions) were collected at room temperature in normal emission with a nonmonochromatized Al Kα X-ray source ($h\nu$ = 1486.6 eV) using 0.1 eV steps, 0.5 s collection time, and 20 eV pass energy. The samples were drop-cast on copper substrates. After drying in air, the obtained films were introduced into the ultrahigh vacuum chamber and outgassed overnight. The XPS photoemission lines were separated into individual components (after Shirley background removal) using symmetrical Voigt functions and nonlinear least-squares routines for the χ^2 minimization.

Linear Optical Spectroscopy. UV-Vis spectra were recorded using a Cary 5 spectrometer (Varian), in the range 200−800 nm. The PL and photoluminescence excitation (PLE) spectra were measured with a FluoroMax-P (Jobin-Yvon) fluorimeter. PL QYs were determined using a relative method following the Demas−Crosby procedure,[36] using Coumarin 153 in ethanol (QY = 56%) and Rhodamine 6G in methanol (QY = 93%) as reference standards.

Fluorescence Correlation Spectroscopy. A frequency-doubled Ti:Sapphire laser (Coherent-Mira900, 76 MHz repetition rate, 150 fs pulse duration) was focused into the CD solution (a mixture of 1:1 water/ethanol) through a water-immersion 60× microscope objective mounted on a confocal microscope system (Olympus-BX51WI/FV300). The laser wavelength was chosen to excite the samples at the maximum of the absorption spectrum. Therefore, for *m*CDs, *o*CDs, and *p*CDs, the wavelength was set to 440 nm, and the average power was modified using neutral density filters. The emission signal, focused on a 100 μm core optical fiber, was split by a 40/60 beam splitter into two avalanche photodiodes (MPD-PDM100). Long-pass filters (450, 450 nm) were employed to reduce the back-scattered laser light in the collection path. Time-correlated single-photon counting, supported by ultrafast electronics (PicoQuant-PicoHarp300), was employed for the calculation of the cross-correlation function to remove after-pulsing artifacts, mainly affecting the curve at short lag times. Each data set is registered with a 180 s collection time. Repeated measurements were run on each sample and the data presented in Figure 2 are averaged fluorescence correlation spectroscopy curves.

Time-Resolved Electron Paramagnetic Resonance (TREPR) spectroscopy. The TREPR spectra were recorded at 80 K on a Bruker Elexsys E680 X-band spectrometer equipped with a nitrogen gas-flow cryostat for sample temperature control. The sample temperature was maintained with an Oxford Instruments CF9350 cryostat and controlled with an Oxford Instruments ITC503. Laser excitation at different wavelengths was provided by an Opotek Opolette Opto-parametric oscillator (OPO) tunable laser (20 Hz repetition rate, E/pulse $\approx$ 4 mJ, λ = 410−700 nm). Laser pulses were depolarized with an achromatic depolarizer. TREPR experiments were performed by direct detection with the transient recorder without lock-in amplification; the microwave power was 0.2 mW. The laser background signal was removed by two-dimensional (2D) baseline correction determined based on the off-resonance transients. The spectra were integrated over 3 μs after the laser flash. An average of 300 transient signals was recorded for all samples at each magnetic field position. TREPR spectral simulations were carried out using the Matlab toolbox Easyspin. The TREPR analysis was performed on *m*CDs, *o*CDs, and *p*CDs in an EtOH solution. In detail, 200 μL of CD solution was poured inside an EPR quartz tube that was sealed under vacuum after several freeze−pump−thaw cycles.

RESULTS AND DISCUSSION

We synthesized three different carbon nanodot systems, henceforth CDs, by solvothermal pyrolysis in ethanol at 180 °C of *ortho*-, *meta*-, and *para*-phenylenediamine (*o*-PD, *m*-PD, and *p*-PD), respectively. These syntheses were proposed in 2015, and owing to the intriguing possibility of obtaining red, green, and blue emitters, the resulting CDs were used for a large number of applications.[4] TEM micrographs prove the successful synthesis of carbon nanoparticles with a large size distribution (Figure 1a). In Figure 1b, we report the size distribution, obtained by statistical analysis. We found average diameters of 13 ± 2, 9.5 ± 3, and 11 ± 2 nm for samples synthesized from *m*-PD, *o*-PD, and *p*-PD, respectively.

https://dx.doi.org/10.1021/acs.jpcc.0c06996
J. Phys. Chem. C 2020, 124, 22314−22320

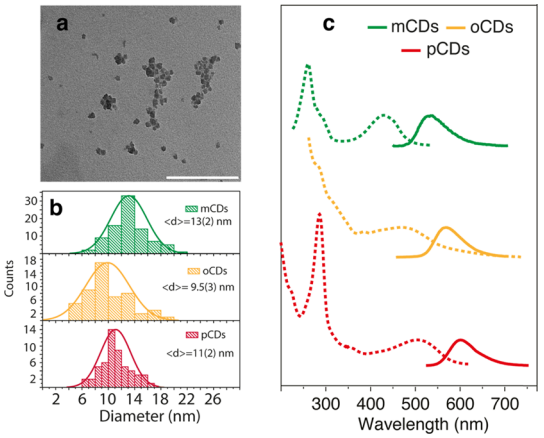

Figure 1. (a) TEM image for as-synthesized *m*CD solutions; scale bar 200 nm. (b) Size distribution histograms from TEM micrographs for the three CD systems. (c) Absorption (dashed) and emission (solid) spectra for purified CD systems. Absorption spectra are normalized on the visible absorption maximum, and emission is normalized to its maximum. Spectra are shifted vertically to assist comparison.

As recently pointed out by Baker et al.,[35] the postsynthesis purification is one of the most crucial steps in the synthesis of CDs, because poor purification strategies are associated with errors and artifacts (e.g., presence of molecular states).[35] Therefore, we studied our samples before and after careful purification by chromatographic separation of the crude.

Thus, following the synthetic procedure from ref 4, we purified the three crude mixtures by silica gel column chromatography. Notably, we were able to isolate emitting fractions in each crude. The purification of each CD yielded an highly fluorescent solution: a red one for *p*-PD-based CDs (*p*CDs), a yellow one for *o*-PD-based CDs (*o*CDs), and a green one for *m*-PD-based CDs (*m*CDs). In Figure 1c, we report the absorption and PL spectra of the purified CD systems. The absorption and emission spectra are analogous to those obtained in ref 4. The absorption spectra display a peaked absorption in the UV region and band in the visible. The maximum of this visible peak shifts from the violet for *m*CDs (430 nm) to (472 nm) and (507 nm) for *o*CDs and *p*CD, respectively. The observed emission bands are broad and largely Stokes shifted (>100 nm) from the absorption ($\lambda_{max,em}$ = 533, 570, and 604 nm for *m*CDs, *o*CDs, and *p*CDs, respectively). Furthermore, as presented in the Supporting Information (Supporting Information Note 1, Figure S1), no excitation-dependent shift could be detected in agreement with ref 4. Photoluminescence excitation (PLE) spectra reveal that this emission originates from the main peaks observed in the absorption spectrum (Figure S1a–c) for all three CD studies. Comparing PLE with absorption spectra of the CDs, we extracted photo-action spectra (PAS) following a procedure that has already been adopted for quantum dots and perovskite nanocrystals.[37,38] We could obtain PL QY excitation spectra through normalization of these PAS with experimentally measured PL QY for the CDs: 0.22 (λ_{ex} = 510 nm), 0.10 (λ_{ex} = 450 nm), and 0.06 (λ_{ex} = 400 nm) for *p*CDs, *o*CDs, and *m*CDs, respectively. Analogously to what was previously observed for citric acid-based CDs, the presence of an excitation wavelength dependence of PL QY spectra (Figure S2d) is indicative of the presence of more than one species with different PL QY values. Specifically, all three CDs show a localized minimum in the PL QY excitation spectrum, around 400 nm for *o*CDs and *p*CDs and around 350 nm for *m*CDs, that suggests the presence of a low PL QY species absorbing in those ranges.

Although the standard investigation on CDs relies on the fundamental inference bridging TEM observations with ensemble optical measurements (i.e., the assumption that the carbon cores observed with TEM are the source of the emission), the observed absence of correlations between size distribution (TEM) and optical properties (PL position) and the inhomogeneity of these optical properties (PL QY excitation spectrum) call into question the role played by quantum confinement invoked by some groups.[39,40] According to the commonly accepted theory, the unifying view on these inconsistencies would rely on the *molecular scaffold model*, describing carbon dots as nanometer-sized carbon spheres decorated with different fluorescent surface groups.[30] Within this framework, the energy transfer interaction between these fluorophores could account for the excitation-independent emission spectrum and for excitation wavelength dependencies in the PL QY. However, here, we sought to solve this conundrum by focusing on the role of molecular species in these systems.

To tackle this puzzling question, we employed fluorescence correlation spectroscopy (FCS), a nonconventional spectroscopic technique, which provides a direct link between the photophysical and structural properties of the material. FCS is based on the analysis of fluorescence intensity fluctuations from femtoliter volumes of a solution.[41,42] Among the wide variety of processes concurring with these fluctuations, we focused on the translational diffusion of the emitters, operating on a micro-to-millisecond time scale.[25] The autocorrelation analysis of the fluorescence signal from the different CD solutions allowed us to estimate the translational diffusion coefficient of the *emitting species*, thereby providing direct access to their average hydrodynamic size. Therefore, we used FCS to circumvent the pitfalls of standard characterization, by directly linking the optical and structural properties of the emitting species.

In Figure 2, we report FCS curves for the three purified CD solutions, in comparison with that from a reference fluorescence standard (Coumarine 503). Already at first glance, it is clear that the relevant time scale of the translational diffusion is similar for all of the CD solutions, as well as the Coumarin standard solution. To account for the presence of

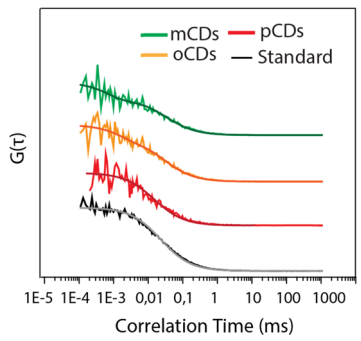

Figure 2. Normalized FCS and fitting curves, for different CDs solutions: *m*CDs (green), *o*CDs (yellow), and *p*CDs (red). Normalization allows an intuitive comparison between diffusional times; fitting was performed prior to normalizing. For the sake of clarity, FCS curves were translated vertically.

https://dx.doi.org/10.1021/acs.jpcc.0c06996
J. Phys. Chem. C 2020, 124, 22314–22320

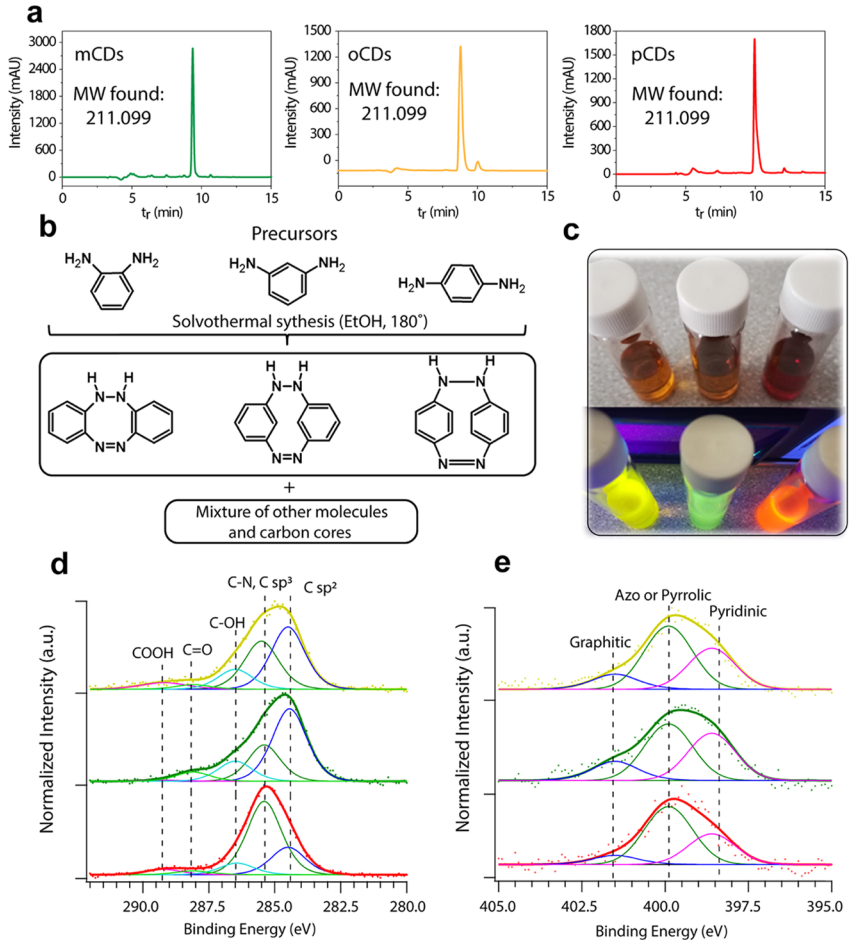

Figure 3. (a) Mass-HPLC showing similar HPLC profiles with identical masses. (b) Chemical structures of *o*-, *m*-, and *p*-diaminobenzene involved in hydrothermal treatments. In the resulting mixtures, three diazo-based cyclic compounds were separated by chromatography (*o*CDs, *m*CDs, and *p*CDs, respectively). (c) *o*CD, *m*CD, and *p*CD samples under vis (up) and UV (bottom) illumination. C 1s (d) and N 1s (e) photoemission lines for *m*CD (green), *o*CD (yellow), and *p*CD (red) samples, as well as the single chemically shifted components from fit deconvolution.

additional slopes on the sub-microsecond time scale (attributed to internal photophysical dynamics), we included a dark-state contribution in the model-fitting FCS curves. A comprehensive description of the model used to fit the FCS curves is given in the SI.[25] The most important parameter gained from this analysis is the translational diffusion time constant τ_D. This time constant is directly associated with the emissive species in the solution. From this, we estimated the hydrodynamic radius of the emissive species via the Stokes–Einstein relation $R_H = \frac{4k_BT\tau_D}{6\pi\eta\omega_0^2}$, where k_B is the Boltzmann constant, T is the temperature, and η is the solution viscosity.[43]

The fitting of FCS curves unequivocally demonstrates that the fluorescence of these samples (*m*CDs, *o*CDs, and *p*CDs) is driven by small species, down to one order of magnitude smaller than the carbon core diameters observed in TEM. Quantitatively, we could estimate an average hydrodynamic radius of R_H = (6.0 ± 0.8, 5.3 ± 0.8, 3.8 ± 0.7 Å) for *m*CDs, *o*CDs, and *p*CDs, respectively. Thus, these measurements prove that the standard characterization (i.e., that relying only on TEM and PL measurements) widely applied for CDs could be misleading in some cases. Despite the direct observation of carbon cores in TEM images, the fluorescence arises mainly from molecules, and the contribution of CDs turns out to be negligible.

To confirm the identity of the emissive species detected by FCS, we studied our samples by HPLC-MS and ^{1}H NMR. As shown in Figure 3a, in each CD solution, we detected similar HPLC profiles with identical masses. ^{1}H–^{1}H COSY NMR (Figure S3) analysis confirms that the observed molecules are the three diazocyclic compounds (Figure 3b) resulting from the three different phenylenediamine isomers. These molecules are likely to result from a variety of reactions occurring during the solvothermal synthesis (i.e., oxidation, self-condensation reactions). The self-adducts of phenylenediamine isomers result in a set of slightly different heteroaromatic molecules, where the delocalization of π electrons varies, and thus accounts for the observed tunable optical properties (Figure 3c). Notably, these molecules belong to the class of indo-dyes, largely used in the textile and hair dye industry owing to their optical properties.[44,45]

The standard chemical analysis (ESI, ^{1}H NMR) cannot determine the presence of the carbon cores. Nevertheless, a possible indication of their presence is given by the X-ray photoemission spectroscopy results. As described in the SI, the C/N (atom/atom) ratio calculated from the surface elemental composition (atom %) determined by XPS quantitative analysis is different for the three samples investigated. The C/N (atom/atom) ratio is 10 for *m*CDs, 7.5 for *p*CDs, and 4.5 for *o*CDs. Compared to the expected CD structure, the higher

https://dx.doi.org/10.1021/acs.jpcc.0c06996
J. Phys. Chem. C 2020, 124, 22314–22320

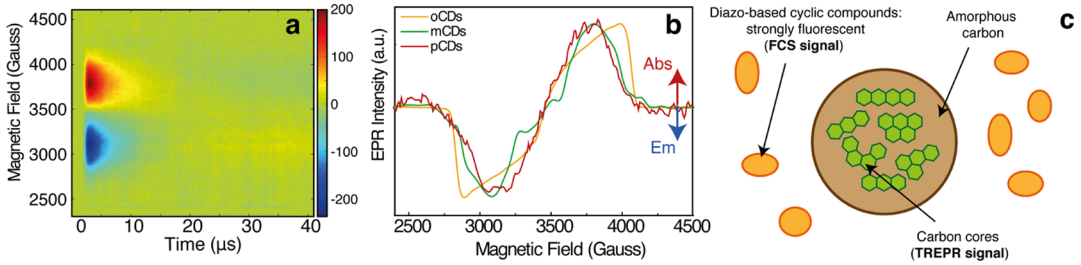

Figure 4. (a) Two-dimensional TREPR spectrum of *m*CDs acquired after a 430 nm laser pulse. (b) One-dimensional TREPR spectra of *m*CDs (green line), *o*CDs (yellow line), and *p*CDs (red line) taken at 3 μs after a monochromatic laser pulse (430 nm for *m*, *o*, and *p*CDs). The measurements were performed at 80 K. Abs, absorption; Em, emission. (c) Schematic representation of the different species discussed in our combined FCS and TREPR spectroscopic analyses, namely, (i) diazo-based cyclic compounds (detected by FCS), (ii) graphene-like sp^2 domains embedded in CDs (detected via TREPR), and (iii) amorphous carbon sp^3 domains within CDs.

value of the C/N ratio calculated from the XPS data is compatible with the presence of additional carbonaceous particles and other nonfluorescent molecular byproducts in the analyzed samples and cannot be attributed solely to the presence of C contamination on the surface of the drop-cast samples. Indeed, C contamination is always present in ex situ prepared samples, but its contribution is expected to be homogeneous for the different analyzed samples since they were prepared simultaneously using the same procedure.[46] Moreover, the differences noticed in the C 1s and N 1s photoemission lines (Figure 3d,e) of the different samples further point toward the presence of carbonaceous particles.[47]

We used time-resolved electron paramagnetic resonance (TREPR) to obtain more accurate information on the nature of carbon cores, as already demonstrated in our previous work.[22] Indeed, there is a consensus about the coexistence of graphene-like sp^2 and amorphous carbon sp^3 domains within the carbon cores. Given that polyaromatic hydrocarbon species have high triplet yields, we used TREPR to extract information on the structure of these transient paramagnetic species inside the carbon cores. The TREPR spectrum of *m*CDs in frozen ethanol solution (80 K) acquired after a 430 nm laser pulse is shown in Figure 4a. Similar spectra were obtained for all of the CD solutions. The spectrum shows broad bands extending for about 1000 gauss with an emissive−absorptive character, a time decay of about 20 μs, and a field position typical of photoexcited triplet states populated by the intersystem-crossing (ISC) mechanism.[48] In Figure 4b, we report the one-dimensional spectra of CDs at a time delay of 3 μs from the laser pulse. To make EPR results compatible with the ones of FCS, the different CDs were excited on their absorption peak. From best-fit spectral simulations (Figures S4−S6), the zero-field splitting (ZFS) parameters, which define the dipolar interaction between the two unpaired electrons of the triplet state, and the relative nonequilibrium populations of the triplet sublevels were obtained (Table S1). The analysis shows the presence of different excited triplet states for each sample, as evidenced by the different ZFS parameters and relative populations. This result highlights the presence of excited triplet states that are delocalized on different species. From the ZFS parameters, it is possible to provide an estimate of the spatial delocalization and the symmetry of the photoexcited triplet states comparing our ZFS values with the values of aromatic and heteroaromatic species tabulated in the literature. The comparison shows that the excited triplet state is delocalized on molecular structures composed of four condensed aromatic rings in all of the samples. To delve deeper into the aromatic structure of the carbon cores, we carried out the same TREPR analysis using different laser wavelengths on purified *m*CDs. The analysis reported in the SI confirms that the observed TREPR signals arise from the sp^2 domains embedded into the carbon cores and highlights the presence of a multitude of different aromatic domains in the carbon cores that can be excited using different wavelengths. Thus, magnetic spectroscopy provides a direct and selective insight into the carbon cores within the CD system. As confirmed by the strong TREPR signal, their high ISC yield suggests that these cores have poor photoluminescence properties.

CONCLUSIONS

In retrospect, this work proves that—at least—a significant fraction of the fluorescence signal observed from CDs does not originate from carbon cores (observed by TEM) or from molecular species linked to them, but rather from small organic molecules in solution. Herein, using fluorescence correlation spectroscopy and analyzing the resulting translational diffusion coefficients for three selected CDs in solution, we can univocally demonstrate the molecular nature of the emissive species in these CDs. These molecules are found to be (i) freely diffusing in the solution and thus not chemically grafted to the carbonaceous core, and (ii) underlying and determining fluorescent properties of CD systems. By employing chemical analysis, we could also demonstrate that these molecules are produced in our synthesis as a self-condensation reaction of phenylenediamine. Lastly, we could indirectly study the carbonaceous cores by observing their triplet states through TREPR.

The conventional characterization of CDs is based on the fundamental bridge linking the structural characterization (e.g., TEM or atomic force microscopy) with the optical characterization (e.g., steady-state fluorescence, time-resolved fluorescence). This procedure is widely employed in nanoscience, but fails here due to the presence of small fluorescent molecules, not detectable by TEM. The dominance of free molecular fluorescence in purified standard CD samples makes more thorough studies on the vast number of available CDs synthesized in the literature urgent. Hence, we believe that the crucial question of whether the observed fluorescence comes from molecular byproducts or a molecular scaffold, or from the carbon cores themselves, should be carefully addressed for every newly synthesized CD system. The methodology reported here will provide essential feedback to organic chemists and will further boost the field of CDs.

https://dx.doi.org/10.1021/acs.jpcc.0c06996
J. Phys. Chem. C 2020, 124, 22314−22320

■ ASSOCIATED CONTENT

Supporting Information

The Supporting Information is available free of charge at https://pubs.acs.org/doi/10.1021/acs.jpcc.0c06996.

Excitation-dependent PL; PLE; XPS discussion; TREPR best-fit details; FCS fitting model; and $^{1}H-^{1}H$ COSY NMR (PDF)

■ AUTHOR INFORMATION

Corresponding Authors

Marcello Righetto − *Department of Chemical Science and U.R. INSTM, University of Padova, I-35131 Padova, Italy;* orcid.org/0000-0001-5507-1445; Email: Marcello.righetto@phd.unipd.it

Camilla Ferrante − *Department of Chemical Science and U.R. INSTM, University of Padova, I-35131 Padova, Italy;* orcid.org/0000-0002-4869-449X; Email: camilla.ferrante@unipd.it

Authors

Francesco Carraro − *Department of Chemical Science and U.R. INSTM, University of Padova, I-35131 Padova, Italy;* orcid.org/0000-0001-8485-4676

Alberto Privitera − *Department of Physics, Oxford University, OX1 3PU Oxford, United Kingdom*

Giulia Marafon − *Department of Chemical Science and U.R. INSTM, University of Padova, I-35131 Padova, Italy*

Alessandro Moretto − *Department of Chemical Science and U.R. INSTM, University of Padova, I-35131 Padova, Italy;* orcid.org/0000-0003-1563-9053

Complete contact information is available at: https://pubs.acs.org/10.1021/acs.jpcc.0c06996

Notes

The authors declare no competing financial interest.

The raw data that support the figures and findings of this paper study are available from corresponding authors upon request.

■ ACKNOWLEDGMENTS

The authors acknowledge the University of Padova (PRAT Prot. N. CPDA155454) for financial support. A.P. thanks the Centre for Advanced Electron Spin Resonance (CAESR), Department of Chemistry, University of Oxford, for the EPR measurements. The work at CAESR was supported by the EPSRC (Grant No. EP/L011972/1). A.P. would also like to thank Prof. Moritz Riede, University of Oxford, for his scientific support and guidance and Dr. William Myers, CAESR facility (Oxford), for his kind assistance with EPR measurements. A.P. acknowledges the European Union's Horizon 2020 research and innovation programme (SEPOMO, Marie Sklodowska Curie, Grant Agreement No. 722651) for funding.

■ REFERENCES

(1) Baker, S. N.; Baker, G. A. Luminescent Carbon Nanodots: Emergent Nanolights. *Angew. Chem., Int. Ed.* **2010**, *49*, 6726−6744.

(2) Li, H.; Kang, Z.; Liu, Y.; Lee, S.-T. Carbon Nanodots: Synthesis, Properties and Applications. *J. Mater. Chem.* **2012**, *22*, 24230−24253.

(3) Righetto, M.; Minotto, A.; Bozio, R. Bridging Energetics and Dynamics of Exciton Trapping in Core−Shell Quantum Dots. *J. Phys. Chem. C* **2017**, *121*, 896−902.

(4) Jiang, K.; Sun, S.; Zhang, L.; Lu, Y.; Wu, A.; Cai, C.; Lin, H. Red, Green, and Blue Luminescence by Carbon Dots: Full-Color Emission Tuning and Multicolor Cellular Imaging. *Angew. Chem., Int. Ed.* **2015**, *54*, 5360−5363.

(5) Privitera, A.; Righetto, M.; Mosconi, D.; Lorandi, F.; Isse, A. A.; Moretto, A.; Bozio, R.; Ferrante, C.; Franco, L. Boosting Carbon Quantum Dots/Fullerene Electron Transfer Via Surface Group Engineering. *Phys. Chem. Chem. Phys.* **2016**, *18*, 31286−31295.

(6) Mosconi, D.; Mazzier, D.; Silvestrini, S.; Privitera, A.; Marega, C.; Franco, L.; Moretto, A. Synthesis and Photochemical Applications of Processable Polymers Enclosing Photoluminescent Carbon Quantum Dots. *ACS Nano* **2015**, *9*, 4156−4164.

(7) Lim, S. Y.; Shen, W.; Gao, Z. Carbon Quantum Dots and Their Applications. *Chem. Soc. Rev.* **2015**, *44*, 362−381.

(8) Wang, Y.; Hu, A. Carbon Quantum Dots: Synthesis, Properties and Applications. *J. Mater. Chem. C* **2014**, *2*, 6921−6939.

(9) Wang, R.; Lu, K.-Q.; Tang, Z.-R.; Xu, Y.-J. Recent Progress in Carbon Quantum Dots: Synthesis, Properties and Applications in Photocatalysis. *J. Mater. Chem. A* **2017**, *5*, 3717−3734.

(10) Hutton, G. A. M.; Martindale, B. C. M.; Reisner, E. Carbon Dots as Photosensitisers for Solar-Driven Catalysis. *Chem. Soc. Rev.* **2017**, *46*, 6111−6123.

(11) Feng, H.; Qian, Z. Functional Carbon Quantum Dots: A Versatile Platform for Chemosensing and Biosensing. *Chem. Rec.* **2018**, *18*, 491−505.

(12) Li, X.; Rui, M.; Song, J.; Shen, Z.; Zeng, H. Carbon and Graphene Quantum Dots for Optoelectronic and Energy Devices: A Review. *Adv. Funct. Mater.* **2015**, *25*, 4929−4947.

(13) Hou, J.; Wang, W.; Zhou, T.; Wang, B.; Li, H.; Ding, L. Synthesis and Formation Mechanistic Investigation of Nitrogen-Doped Carbon Dots with High Quantum Yields and Yellowish-Green Fluorescence. *Nanoscale* **2016**, *8*, 11185−11193.

(14) Miao, X.; Qu, D.; Yang, D.; Nie, B.; Zhao, Y.; Fan, H.; Sun, Z. Synthesis of Carbon Dots with Multiple Color Emission by Controlled Graphitization and Surface Functionalization. *Adv. Mater.* **2018**, *30*, No. 1704740.

(15) Essner, J. B.; Baker, G. A. The Emerging Roles of Carbon Dots in Solar Photovoltaics: A Critical Review. *Environ. Sci. Nano* **2017**, *4*, 1216−1263.

(16) Du, Q.; Zheng, J.; Wang, J.; Yang, Y.; Liu, X. The Synthesis of Green Fluorescent Carbon Dots for Warm White Leds. *RSC Adv.* **2018**, *8*, 19585−19595.

(17) Zhu, S.; Song, Y.; Zhao, X.; Shao, J.; Zhang, J.; Yang, B. The Photoluminescence Mechanism in Carbon Dots (Graphene Quantum Dots, Carbon Nanodots, and Polymer Dots): Current State and Future Perspective. *Nano Res.* **2015**, *8*, 355−381.

(18) Zhu, S.; Wang, L.; Li, B.; Song, Y.; Zhao, X.; Zhang, G.; Zhang, S.; Lu, S.; Zhang, J.; Wang, H.; et al. Investigation of Photoluminescence Mechanism of Graphene Quantum Dots and Evaluation of Their Assembly into Polymer Dots. *Carbon* **2014**, *77*, 462−472.

(19) Verma, N. C.; Yadav, A.; Nandi, C. K. Paving the Path to the Future of Carbogenic Nanodots. *Nat. Commun.* **2019**, *10*, No. 2391.

(20) Zhu, P.; Tan, K.; Chen, Q.; Xiong, J.; Gao, L. Origins of Efficient Multiemission Luminescence in Carbon Dots. *Chem. Mater.* **2019**, *31*, 4732−4742.

(21) Chen, Q.; Zhu, P.; Xiong, J.; Gao, L.; Tan, K. A New Dual-Recognition Strategy for Hybrid Ratiometric and Ratiometric Sensing Perfluorooctane Sulfonic Acid Based on High Fluorescent Carbon Dots with Ethidium Bromide. *Spectrochim. Acta, Part A* **2020**, *224*, No. 117362.

(22) Song, Y.; Zhu, S.; Zhang, S.; Fu, Y.; Wang, L.; Zhao, X.; Yang, B. Investigation from Chemical Structure to Photoluminescent Mechanism: A Type of Carbon Dots from the Pyrolysis of Citric Acid and an Amine. *J. Mater. Chem. C* **2015**, *3*, 5976−5984.

(23) Schneider, J.; Reckmeier, C. J.; Xiong, Y.; von Seckendorff, M.; Susha, A. S.; Kasák, P.; Rogach, A. L. Molecular Fluorescence in Citric Acid-Based Carbon Dots. *J. Phys. Chem. C* **2017**, *121*, 2014−2022.

(24) Sharma, A.; Gadly, T.; Gupta, A.; Ballal, A.; Ghosh, S. K.; Kumbhakar, M. Origin of Excitation Dependent Fluorescence in Carbon Nanodots. *J. Phys. Chem. Lett.* **2016**, *7*, 3695−3702.

(25) Righetto, M.; Privitera, A.; Fortunati, I.; Mosconi, D.; Zerbetto, M.; Curri, M. L.; Corricelli, M.; Moretto, A.; Agnoli, S.; Franco, L.; et al. Spectroscopic Insights into Carbon Dot Systems. *J. Phys. Chem. Lett.* **2017**, 2236−2242.
(26) Sharma, A.; Gadly, T.; Neogy, S.; Ghosh, S. K.; Kumbhakar, M. Molecular Origin and Self-Assembly of Fluorescent Carbon Nanodots in Polar Solvents. *J. Phys. Chem. Lett.* **2017**, *8*, 1044−1052.
(27) Khan, S.; Sharma, A.; Ghoshal, S.; Jain, S.; Hazra, M. K.; Nandi, C. K. Small Molecular Organic Nanocrystals Resemble Carbon Nanodots in Terms of Their Properties. *Chem. Sci.* **2018**, *9*, 175−180.
(28) Shi, L.; Yang, J. H.; Zeng, H. B.; Chen, Y. M.; Yang, S. C.; Wu, C.; Zeng, H.; Yoshihito, O.; Zhang, Q. Carbon Dots with High Fluorescence Quantum Yield: The Fluorescence Originates from Organic Fluorophores. *Nanoscale* **2016**, *8*, 14374−14378.
(29) Qu, D.; Zheng, M.; Zhang, L.; Zhao, H.; Xie, Z.; Jing, X.; Haddad, R. E.; Fan, H.; Sun, Z. Formation Mechanism and Optimization of Highly Luminescent N-Doped Graphene Quantum Dots. *Sci. Rep.* **2014**, *4*, No. 5294.
(30) Fu, M.; Ehrat, F.; Wang, Y.; Milowska, K. Z.; Reckmeier, C.; Rogach, A. L.; Stolarczyk, J. K.; Urban, A. S.; Feldmann, J. Carbon Dots: A Unique Fluorescent Cocktail of Polycyclic Aromatic Hydrocarbons. *Nano Lett.* **2015**, *15*, 6030−6035.
(31) Demchenko, A. P.; Dekaliuk, M. O. The Origin of Emissive States of Carbon Nanoparticles Derived from Ensemble-Averaged and Single-Molecular Studies. *Nanoscale* **2016**, *8*, 14057−14069.
(32) Das, A.; Roy, D.; De, C. K.; Mandal, P. K. "Where Does the Fluorescing Moiety Reside in a Carbon Dot?" − Investigations Based on Fluorescence Anisotropy Decay and Resonance Energy Transfer Dynamics. *Phys. Chem. Chem. Phys.* **2018**, *20*, 2251−2259.
(33) Xiong, Y.; Schneider, J.; Ushakova, E. V.; Rogach, A. L. Influence of Molecular Fluorophores on the Research Field of Chemically Synthesized Carbon Dots. *Nano Today* **2018**, *23*, 124−139.
(34) Mishra, K.; Koley, S.; Ghosh, S. Ground-State Heterogeneity Along with Fluorescent Byproducts Causes Excitation-Dependent Fluorescence and Time-Dependent Spectral Migration in Citric Acid-Derived Carbon Dots. *J. Phys. Chem. Lett.* **2019**, *10*, 335−345.
(35) Essner, J. B.; Kist, J. A.; Polo-Parada, L.; Baker, G. A. Artifacts and Errors Associated with the Ubiquitous Presence of Fluorescent Impurities in Carbon Nanodots. *Chem. Mater.* **2018**, *30*, 1878−1887.
(36) Crosby, G. A.; Demas, J. N. Measurement of Photoluminescence Quantum Yields. Review. *J. Phys. Chem. A* **1971**, *75*, 991−1024.
(37) Righetto, M.; Lim, S. S.; Giovanni, D.; Lim, J. W. M.; Zhang, Q.; Ramesh, S.; Tay, Y. K. E.; Sum, T. C. Hot Carriers Perspective on the Nature of Traps in Perovskites. *Nat. Commun.* **2020**, *11*, No. 2712.
(38) Li, B.; Brosseau, P. J.; Strandell, D. P.; Mack, T. G.; Kambhampati, P. Photophysical Action Spectra of Emission from Semiconductor Nanocrystals Reveal Violations to the Vavilov Rule Behavior from Hot Carrier Effects. *J. Phys. Chem. C* **2019**, *123*, 5092−5098.
(39) Qu, D.; Zheng, M.; Li, J.; Xie, Z.; Sun, Z. Tailoring Color Emissions from N-Doped Graphene Quantum Dots for Bioimaging Applications. *Light Sci. Appl.* **2015**, *4*, No. e364.
(40) Zhu, S.; Song, Y.; Wang, J.; Wan, H.; Zhang, Y.; Ning, Y.; Yang, B. Photoluminescence Mechanism in Graphene Quantum Dots: Quantum Confinement Effect and Surface/Edge State. *Nano Today* **2017**, *13*, 10−14.
(41) Schwille, P.; Haustein, E. Fluorescence Correlation Spectroscopy: An Introduction to Its Concepts and Applications, In *Biophysics Textbook Online* 2002.
(42) Ries, J.; Schwille, P. Fluorescence Correlation Spectroscopy. *BioEssays* **2012**, *34*, 361−368.
(43) Fortunati, I.; Weber, V.; Giorgetti, E.; Ferrante, C. Two-Photon Fluorescence Correlation Spectroscopy of Gold Nanoparticles under Stationary and Flow Conditions. *J. Phys. Chem. C* **2014**, *118*, 24081−24090.
(44) Robbins, C. R. Dyeing Human Hair, In *Chemical and Physical Behavior of Human Hair*, Robbins, C. R., Ed.; Springer Berlin Heidelberg: Berlin, Heidelberg, 2012; pp 445−488.
(45) Corbett, J. F. An Historical Review of the Use of Dye Precursors in the Formulation of Commercial Oxidation Hair Dyes. *Dyes Pigm.* **1999**, *41*, 127−136.
(46) Carraro, F.; Cattelan, M.; Favaro, M.; Calvillo, L. Aerosol Synthesis of N and N-S Doped and Crumpled Graphene Nanostructures. *Nanomaterials* **2018**, *8*, 406.
(47) Favaro, M.; Carraro, F.; Cattelan, M.; Colazzo, L.; Durante, C.; Sambi, M.; Gennaro, A.; Agnoli, S.; Granozzi, G. Multiple Doping of Graphene Oxide Foams and Quantum Dots: New Switchable Systems for Oxygen Reduction and Water Remediation. *J. Mater. Chem. A* **2015**, *3*, 14334−14347.
(48) Righetto, M.; Privitera, A.; Carraro, F.; Bolzonello, L.; Ferrante, C.; Franco, L.; Bozio, R. Engineering Interactions in QDs−PCBM Blends: A Surface Chemistry Approach. *Nanoscale* **2018**, *10*, 11913−11922.

https://dx.doi.org/10.1021/acs.jpcc.0c06996
J. Phys. Chem. C 2020, 124, 22314−22320